JOURNAL OF MATERIALS SCIENCE: MATERIALS IN MEDICINE **10** (1999) 275–281

Corrosion and biocompatibility of orthodontic wires

F. WIDU, D. DRESCHER
Department of Orthodontics, Heinrich-Heine-Universität, Düsseldorf, Germany
R. JUNKER, C. BOURAUEL
Department of Orthodontics, Friedrich-Wilhelms-Universität, Bonn, Germany

With the increasing number of orthodontic treatments using devices containing nickel and the growing prevalence of nickel allergy in the average population, biocompatibility studies of these devices have become a topic of major interest. The corrosion behavior of orthodontic wires is a decisive factor determining their biocompatibility. Therefore four nickel–titanium guiding arches, a titanium–molybdenum and a stainless steel wire were analyzed for corrosion behavior under realistic conditions. Pure potentiostatic, pure mechanical and combined potentiostatic and mechanical stresses were applied to the specimens. Subsequently, the surfaces of the wires were investigated employing atomic force microscopy (AFM) and nickel loss was measured with an atomic absorption spectrophotometer. The results yield information about the relative corrosion tendency of the wires under *in vitro* conditions. The wires examined can be classified into two groups, one with a high and a second group with a low tendency towards corrosion, that is American Orthodontics Memory wire as well as GAC Neo Sentalloy and Ormco Ni–Ti as well as Unitek Nitinol respectively. Although corrosion behavior under clinical conditions can not be directly derived from these results, analyses of wires after clinical usage indicate that changes of wire surfaces might show the same characteristics under *in vitro* conditions.

1. Introduction

Development of orthodontic devices is closely related to innovations in the science of materials. A significant advance in orthodontic materials was achieved in 1971 with the introduction of wires made of nickel–titanium (NiTi) alloys into clinical practice [1]. In a near equi-atomic composition NiTi alloys reveal exceptional mechanical characteristics such as shape memory effect and superelasticity. Especially the latter physical property is the feature that led to new treatment advantages in the correction of malpositions of teeth. NiTi alloys offer the possibility to design orthodontic devices with lighter and almost constant forces and with a greater working range as conventional stainless steel devices. An ideal superelastic NiTi wire is characterized by a stress/strain curve displaying a broad hysteresis with quasi-horizontal plateau branches (Fig. 1). Thus, a nearly constant stress of the material over a wide range of strain is observed. Superelasticity as well as the shape memory effect are based on the special crystaline structure of NiTi alloys with a phase transformation from martensite to austenite and vice versa under cyclic or thermal load [2].

Due to its extraordinary mechanical properties, the employment of orthodontic devices made of NiTi alloys has reached a high level of acceptance over the past two decades. On the other hand a number of papers deal with the susceptibility of NiTi wires to corrosion [3-5]. *In vitro*, as well as *in vivo*, analysis of NiTi wires revealed the occurence of pitting corrosion. For this reason NiTi wires are characterized as being less corrosion resistant than cobalt–chromium or titanium–molybdenum wires and the passivating layer of NiTi may be less stable than that of the standard alloys [4]. Corrosion processes are presumed to have negative consequences on biocompatibility, aesthetic appearance and on treatment progress caused by the influence of friction on sliding mechanics. Simultaneous corrosion and mechanical stresses during mastication may affect the deflection properties of NiTi wires [6, 7]. However, there is no total agreement on this topic. Several authors evaluate the corrosion behavior of NiTi and stainless steel wires as being equal [8-10].

A material is defined as being biocompatible if it has no negative influences on its biological environment, i.e. no toxic, allergic or carcinogenic reactions can be observed. In addition, the physical properties of the material should not be affected during *in vivo* usage. In the special case of an alloy, the alloy itself and all of its components have to be examined under allergic, toxic and carcinogenic aspects as the loss of each component is possible by corrosion processes and abrasion. As a

Author for correspondence: Dr Christoph Bourauel, Poliklinik für Kieferorthopädie, Rheinische Friedrich-Wilhelms-Universität Bonn, Welschnonnenstr. 17, 53111 Bonn, Germany

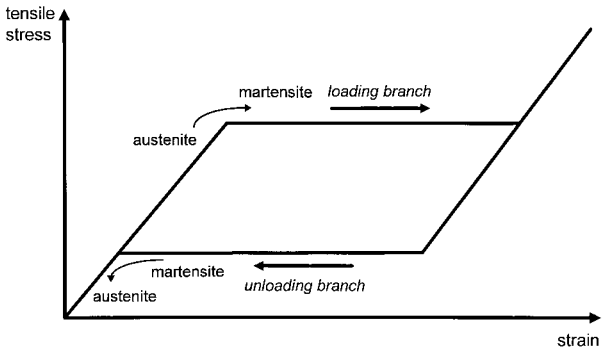

Figure 1 Stress/strain curve of an idealistic superelastic NiTi wire. Maximum strain is about 10%, plateau regimes start between 0.5% and 1.5% of relative strain and end at 4.0–6.5%.

consequence, contact of ions with surrounding tissue as well as distribution into the organism may occur. Titanium is classified as being highly biocompatible, nickel as being uncompatible and toxic. Nickel is a very potent allergen and causes hypersensitivity reactions to a greater extent than any other metal or alloy [11]. The IARC (International Agency for Research on Cancer) evaluated metallic nickel as being possibly carcinogenic and nickel compounds as being carcinogenic [12].

Only a few, not very unanimous, experimental results are documented on biocompatibility of NiTi wires. Cytotoxicity tests showed cell growth to be affected by NiTi wires [13]. The possibility of nickel sensitivity being induced in a patient by NiTi wire has not been clarified yet. In lymphocyte transformation tests orthodontic devices lost a sufficient amount of nickel in a chemical form that is able to cause proliferation of lymphocytes [14]. Thus, patients who are already sensitized to nickel can show allergic reactions caused by nickel loss from orthodontic devices. The above-mentioned study could not classify wires into different corrosion categories, as whole fixed appliances were investigated. Several authors recommend the use of nickel-free devices for the treatment of patients, who are already extremely sensitized to nickel, as cases of allergic reactions to nickel containing orthodontic devices have already been reported [15, 16, 17]. On the other hand, there is no clinical evidence to support the theory of orthodontic NiTi wires as being potentially carcinogenic.

Growing numbers of orthodontic treatments and the increasing prevalence of nickel allergy in the population require a minimization of the nickel loss from NiTi wires in the oral cavity. Even wires of the same alloy but from different manufacturers show a variety of characteristics with regard to structure, homogeneity and surface roughness [18, 19]. This indicates that corrosion behavior might differ between different orthodontic NiTi wires as well. It was the aim of this study to characterize the corrosion behavior of NiTi wires *in vitro*, simulating the intra-oral environment in a nearly realistic manner. The results should be helpful for the further development of orthodontic devices under the aspects of biocompatibility.

2. Materials and methods

2.1. Materials

The study focused on four orthodontic NiTi wires, where two could be classified as being superelastic (Titanium Memory Wire and Neo Sentalloy) and two were of the highly elastic type (Nitinol and Ormco Ni-Ti). A titanium–molybdenum and one stainless steel wire were included in the study in order to enable a comparison of the NiTi wires with these orthodontic standard materials. Table I lists information about the chemical composition and manufacturers of all wires investigated. The guiding arches were tested exclusively in the dimension 0.406×0.559 mm to establish standard test conditions. The wires chosen give an overview of the current market.

2.2. General experimental procedure

The corrosion behavior of orthodontic wires was tested by exposure to anodic polarization and to mechanical stresses in a modified Fusayama saliva. A first characterization of the wires was made by recording current densities versus polarization potentials to obtain rupture potentials. Subsequently the wires were examined with an atomic force microscope (AFM). To obtain quantitative information on the surface changes the average mean surface roughness, (R_a), was calculated from the surface scans with the AFM. Nickel loss, i.e. nickel that was dissolved into the artificial saliva, was measured with an atomic absorption spectrometer. Lastly a NiTi wire (Nitinol) was examined with the AFM after clinical usage to compare its surface characteristics with the laboratory results.

2.3. Electrochemical cell

An electrochemical cell (Fig. 2) was constructed with a Ag/AgCl reference electrode (Type B 2820, Schott, Germany), a platinum counter electrode, a Haber–Luggin capillary (salt bridge), a gas inlet/outlet for N_2 rinsing and a temperature controlling system. The electrochemical cell was driven by a specially

TABLE I Orthodontic wires used in this study (chemical composition given in atomic % [17])

Product	Manufacturer	Alloy	Chemical composition
Titanium Memory Wire	American Orthodontics	Nickel–titanium	52% Ni, 48% Ti
Neo Sentalloy	GAC International	Nickel–titanium	52.9% Ni, 47.1% Ti
Ni-Ti	Ormco	Nickel–titanium	52.4% Ni, 47.6% Ti
Nitinol	3M/Unitec	Nickel–titanium	52% Ni, 45% Ti, 3% Cr
TMA	Ormco	Titanium–molybdenum	78% Ni, 11% Mo, 6% Zr, 4.5% Sn
Stainless Steel	3M/Unitec	Stainless steel	72.0%Fe, 18% Cr, 8% Ni

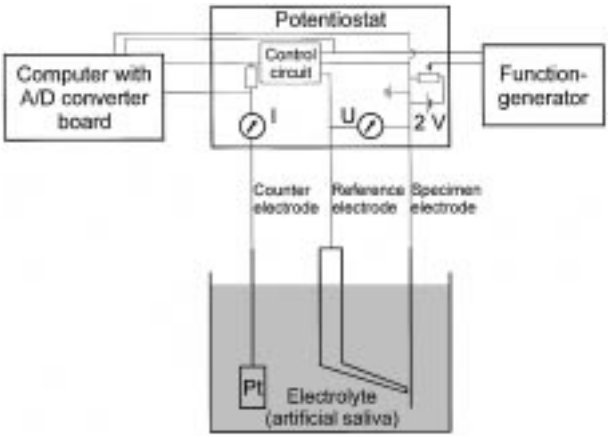

Figure 2 Schematic experimental set-up of the electrochemical cell used.

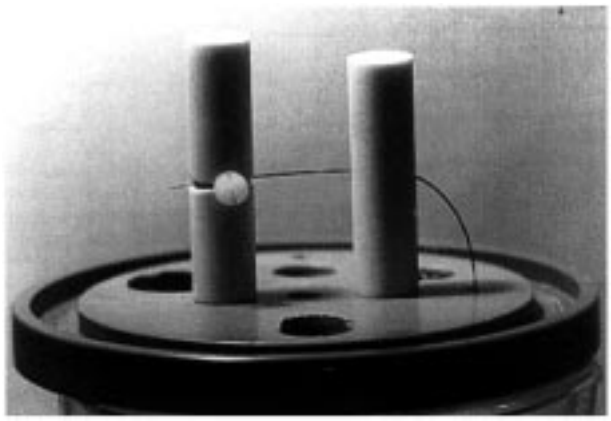

Figure 3 Inert macor appliance used for fixing of the wires in the electrochemical cell.

constructed potentiostate (electronics workshop, Department of Chemical Physics, University of Bonn) and a function generator (TG 230, Thurlby-Thandar, UK). Additionally a vertically moveable inert glass rod was integrated for mechanical load application. The set-up was controlled and data was taken by a personal computer via an A/D converter board.

A defined length of 3 cm of each of the specimens was exposed as electrode to the electrolyte. Modified Fusayama artificial saliva [20] at 37 °C was chosen as the electrolyte as it tends to correlate best in corrosion experiments with the results obtained from natural saliva [21]. The composition of the saliva used is listed in Table II. To determine the rupture potentials, anodic potentiodynamic and potentiostatic polarization were performed for a first classification of the wires. The specimens were subjected to a potentiostatic polarization of 0.72 and 1.22 mV (NHE) in order to accelerate the natural corrosion process which is very slow. Each specimen was polarized for 60 s at the above-mentioned values. A reaction between the wire and the electrolyte can be observed when the polarization value is higher than the rupture potential of the specimen.

In a second experimental series wires were exposed to mechanical stresses to simulate the intra-oral situation during mastication. 10 000 bending cycles were carried out with a glass rod that moved vertically over a distance of 1.5 mm with a frequency of 1 Hz. The wires were fixed in the electrolyte with a free wire length of 3 cm by macor rods with specialized wire clamps (Fig. 3). This is a typical free bending length comparable to the space between two teeth around an extraction site. Subsequently surface scans were taken again with the AFM and the mean roughness R_a was calculated. In a third series mechanical stresses were combined with potentiostatic polarization for each specimen and again surface characteristics were evaluated.

In the closing part of the study the wires were polarized for 10 min at 0.72 and 1.22 V/NHE in the artificial Fusayama saliva, the resulting precipitates were homogenized in an ultrasonic bath and the amount of dissolved nickel was determined with an atomic absorbtion spectrophotometer (Perkin-Elmer, Norwalk, CT, USA). The linear working range of the spectrometer selected equates the maximum observed nickel concentration; thus the measured values of the samples with smallest nickel content have a significantly higher error.

TABLE II Compsition of the artificial Fusayama saliva used in this study

Component	(mg l^{-1})
Sodium chloride	400
Potassium chloride	400
Calcium chloride-dihydrate	795
Sodium hydrogen phosphate-1-hydrate	690
Potassium rhodanide	300
Sodium sulfide	5
Urea	1000

2.4. Atomic force microscopy

The atomic force microscope (AFM) [22] belongs to a new class of non-destructive microscopes for surface analysis called scanning probe microscopes. The AFM is able to perform surface analysis without direct interaction with the specimen's surface. The AFM delivers three-dimensional realistic impressions of the scanned surfaces. Scanned areas reach from atomic level up to 140 μm square. No extensive preparation of the specimen is required, which makes AFM a labor saving, fast method. From these surface scans of the specimens a large variety of surface characteristics can be derived and the average mean surface roughness was chosen to compare the different wires.

The generation of surface scans is performed with a very fine tip (radius of curvature 20–40 nm) located at the end of a cantilever (length and thickness about 200 μm and 0.5 μm respectively, see Fig. 4). The tip approaches the specimen's surface and at a distance of approximately 100 nm Coulombian forces cause the cantilever to bend. A laser beam being reflected from the back of the bent cantilever is registered by a segmented photodiode and each movement of the cantilever causes a shift of the light spot out of the center of the photodiode. This information is used to keep the distance between specimen and tip constant by controlling the vertical position of the probe via piezo-driven positioning devices. Surfaces are scanned in subsequent lines to record the whole surface topography. A commercial

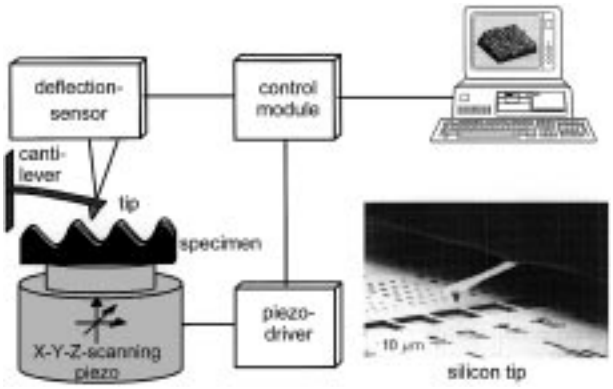

Figure 4 Sketch of an atomic force microscope.

AFM Nanoscope III from Digital Instruments Inc. (San Diego, USA) was used. The method is limited to vertical scanning ranges of about 5 µm. Thus, as several samples showed massive pitting corrosion after polarization, these wires were measured additionally with an electron microscope (JSM T300, Jeol).

3. Results

3.1. Rupture potentials

Table III lists the results of all analyses. The rupture potential of the titanium–molybdenum wire could not be determined. Even polarization over a period of 12 h at a polarization potential of 2.22 V/NHE did not cause any material loss. All other products could be classified into a group with a higher rupture potential (i.e. $U > 600$ mV/NHE) and a group with a lower rupture potential (i.e. $U < 600$ mV/NHE).

3.2. AFM analysis, atomic absorption spectrometry

Fig. 5 depicts examples of the AFM scans of all wires examined. The top view of 100 µm square is a result of digital image processing. The samples were measured in as-received state. Each specimen has its own characteristic surface structure. Typical grooves caused by the production process are visible on all wires except the Neo Sentalloy which seems to be the roughest.

Fig. 6a and b show three-dimensional views of the Titanium Memory wire. The height is displayed in a larger scale to better illustrate the surface structure. Fig. 6a depicts the unpolarized surface of this wire, which is very smooth and homogeneous except for some grooves.

TABLE III Rupture potentials determined for all wires in this study

Wire	Rupture potential (mV)
Titanium Memory wire	320–370
Neo Sentalloy	370–420
Ni–Ti	720–770
Nitinol	720–770
TMA	–
Stainless steel	620–670

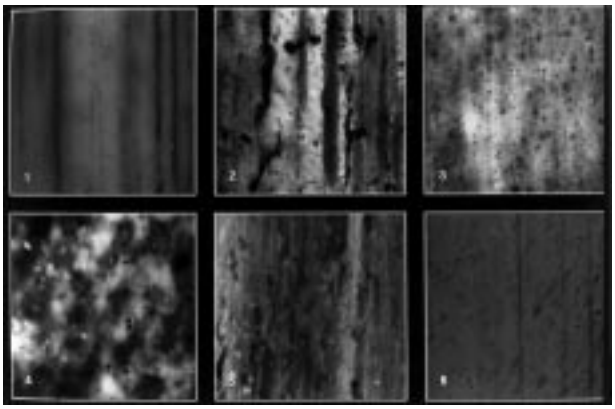

Figure 5 Surface scans of all wires examined. Top view at 100 × 100 µm. 1 Titanium Memory wire; 2 Neo Sentalloy; 3 Ni–Ti; 4 Nitinol; 5 TMA; 6 Stainless steel.

After a 1 min potentiostatic polarization at 1.22 V/NHE a combination of pitting and area corrosion could be observed. Scanning of the surface of the polarized Titanium Memory with the AFM could only be performed in smoother areas due to the high vertical variations caused by corrosion. Thus corrosion processes were documented additionally with an electron microscope (Fig. 7a and b, magnification × 350 and × 2000, respectively). The pictures show massive pitting corrosion but the true depth of the structures could not be determined.

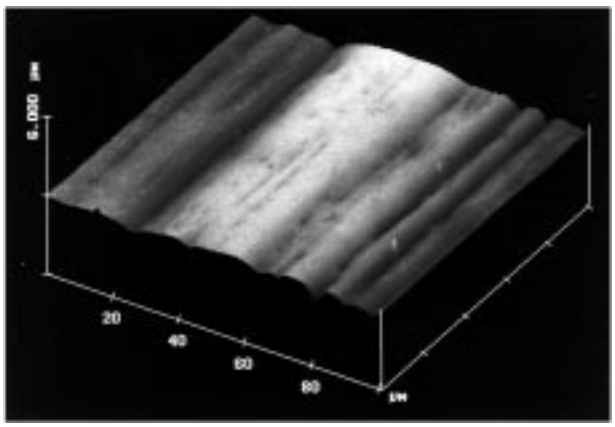

(a)

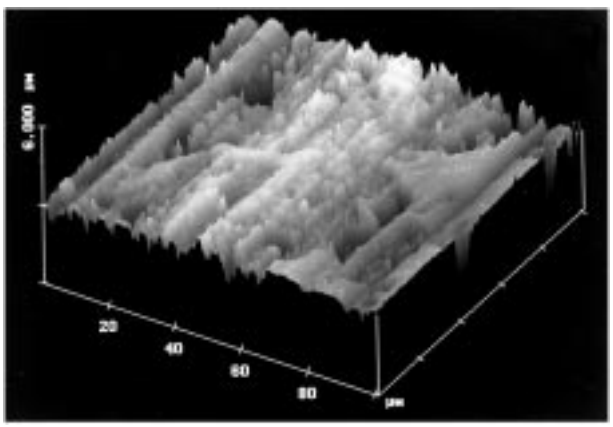

(b)

Figure 6 (a) 3D view of a 100 × 100 µm surface scan taken with the AFM from the Titanium Memory wire in as-received state. (b) Surface of the same wire after potentiostatic polarization of 1 min at 1.22 V/NHE.

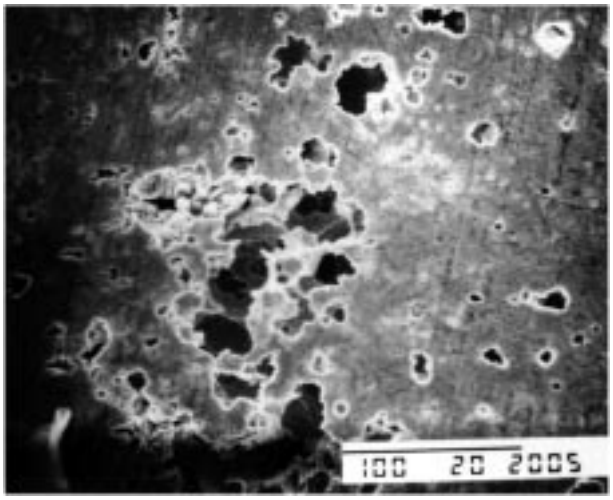

(a)

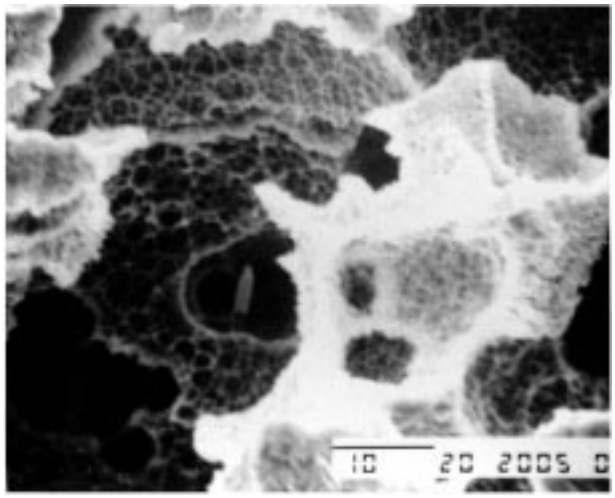

(b)

Figure 7 (a) Polarized titanium memory wire. Scan taken with the electron microscope, magnification × 350. (b) Same wire at a magnification of × 2000. Destruction of the surface due to pitting corrosion is quite obvious.

Fig. 8a depicts a surface scan of the as-received Nitinol wire. Scaling is similar to Fig. 6. The unpolarized sample of Nitinol is much rougher than that of the Titanium Memory wire. Nevertheless, surface defects after clinical use are comparable to corrosion processes of the Titanium Memory wire due to polarization. This can be seen from Fig. 8b, which shows an AFM scan of a Nitinol wire that remained over a period of 3 months in a patient's mouth.

Table IV summarizes the surface roughness and nickel loss determined for all wires. The values are the mean of 10 measurements, standard deviation is given in parentheses. The smoothest wires in as-received state are the Titanium Memory wire and the stainless steel, all other products are much rougher. Comparing the surface roughness of the unpolarized wires with the polarized ones the R_a value only increases significantly for the Titanium Memory wire. There are no significant changes of the R_a value after polarization for all other wires. Measured nickel dissolution in the artificial saliva was highest for the Titanium Memory wire which correlates very well with the changes of the surface structure by polarization. The second largest nickel loss was determined for Neo Sentalloy, but a correlation with

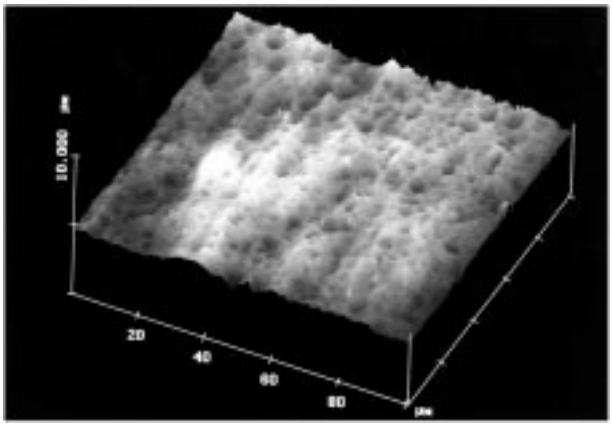

(a)

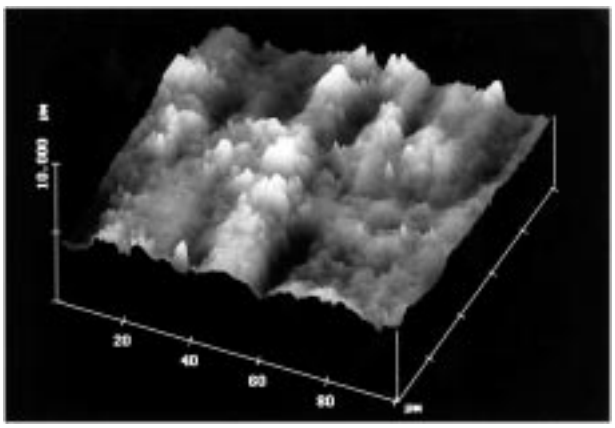

(b)

Figure 8 (a) Surface scan taken with the AFM from the Nitinol wire in as-received state. (b) Surface scan (AFM) of a Nitinol wire after a period of 3 months in the patient's mouth.

changes in the R_a value could not be ascertained. All other wires showed no significant nickel loss. Combined mechanical and electrochemical stresses did not have any effect on corrosion behavior, surface structure or nickel loss compared to pure potentiostatic stress.

4. Discussion

Orthodontic NiTi wires show differences in their corrosion behavior. Resultantly the products analyzed can be split into two categories. Rupture potentials and nickel loss in combination with changes of the surface roughness were taken into account as indicators of their tendency towards corrosion.

The first group is characterized by low rupture potentials (i.e. below 600 mV/NHE), has a high tendency towards corrosion and is composed of the Titanium Memory wire and Neo Sentalloy. The Titanium Memory wire showed drastic changes of surface topography after potentiostatic stress. Pitting and area corrosion were detected with the AFM. R_a values changed significantly. The changes in surface structure correlated with nickel dissolution in the electrolyte (artificial saliva), that was more than 100 times greater than the smallest one. Changes in surface structure were quite small for the Neo Sentalloy but the nickel loss determined was greater by a factor of 10–20 in comparison with the other group.

The second category is represented by wires with low corrosion tendency. The Ni–Ti wire and the Nitinol from

TABLE IV Summary of the results

Product	Alloy	R_a Unstressed (nm)	R_a (1 min)		Ni concentration (10 min)	
			0.72 V/NHE (nm)	1.22 V/NHE (nm)	0.72 V/NHE ($mg\,l^{-1}$)	1.22 V/NHE ($mg\,l^{-1}$)
Titanium Memory wire	Nickel–titanium	110 (25)	180 (60)	>290 (180)	23.0	39.4
Neo Sentalloy	Nickel–titanium	325 (30)	335 (80)	340 (35)	3.1	17.7
Ni–Ti	Nickel–titanium	335 (100)	260 (65)	215 (25)	0.2	0.2
Nitinol	Nickel–titanium	325 (70)	355 (75)	385 (55)	0.1	0.3
TMA	Titanium–molybdenum	340 (80)	270 (60)	425 (170)	–	–
Stainless steel	Stainless steel	80 (35)	65 (10)	55 (10)	0.4	0.7

the nickel–titanium products, as well as the TMA and the stainless steel wire from the reference group belong to this category. The rupture potentials of these samples were higher (i.e. above 600 mV/NHE) and no significant changes in surface structure or in the R_a value after potentiostatic polarization could be determined. On the contrary, a smoothing of the surface was determined for the NiTi wires and stainless steel. This might be explained by a flattening of the peaks and troughs that resulted from production. The nickel loss from the wires in this group was much smaller than the one from the wires in the first group. Especially, the TMA wire was chemically inert. A rupture potential could not be detected and due to its composition nickel loss could not be expected.

Several factors are responsible for varying corrosion behaviors of the specimen wires. A highly important one is the alloy composition although the different tendencies towards corrosion cannot be directly derived from the alloy composition, which is nearly identical for all NiTi wires. However, AFM scanning revealed that each wire has a typical surface structure resulting from different production and especially finishing processes. The influence of surface corrugation and structural constitution might be a reason for varying corrosion tendency. However, the present study is not able to answer the question as to which one of the stated factors is the most important in determining the differing tendency towards corrosion of the various orthodontic NiTi wires. Additionally a transfer of the laboratory results to the intra-oral situation is impossible as potentiostatic loads in the mouth are much smaller than under laboratory conditions.

Thus, only a categorization of the samples could be achieved and the determined corrosion behavior of the products analyzed must be understood as being relative among the samples. Consequently the expressions high and low corrosion tendency are not absolute ratings, although the changes in the surface structure of a Nitinol wire after clinical usage indicate that the resulting processes in the mouth are comparable to *in vitro* processes.

5. Conclusions

The categorization of the corrosion behavior is not implicitly a categorization of the biocompatibility of the analyzed wires. The results of the present *in vitro* study can not be transferred unrestrictedly to clinical conditions. There are many more factors than corrosion that have an influence on biocompatibility. It is important to discover which surface structures start the corrosion process or which structures enhance the corrosion defects. An *in situ* analysis of corrosion process via AFM and a connected electrochemical cell is planned. The results of this experimental set-up could help to optimize production processes and to clarify the effects of interaction between alloy composition, crystal structure and surface corrugation on corrosion behavior. These are not yet totally understood. Another aspect of optimization is the reduction of surface roughness. This will have a positive effect on treatment progress, aesthetic appearance and plaque retention.

Acknowledgment

The authors wish to thank the Minister für Wissenschaft und Forschung, Nordrhein-Westfalen for financial support.

References

1. G. F. ANDREASEN and T. B. HILLEMAN, *J. Am. Dent. Assoc.* **82** (1971) 1373.
2. W. J. BUEHLER, J. V. GILFRICH and R. C. WILEY, *J. Appl. Phys.* **34** (1963) 1457.
3. K. CLINARD, J. A. VON FRAUENHOFER and M. M. KUFTINEC, *J. Dent. Res.* **60** (1981) 682.
4. N. K. SARKAR, W. REDMOND, B. SCHWANINGER and A. J. GOLDBERG, *J. Oral. Rehab.* **10** (1983) 121.
5. N. K. SARKAR and B. SCHWANINGER, *J. Dent. Res.* **59** (1980) 528 (Abstract).
6. E. F. HARRIS, S. M. NEWMAN and J. A. NICHOLSON, *Am. J. Orthod. Dentofac. Orthop.* **93** (1988) 508.
7. A. HARTEL, C. BOURAUEL, D. DRESCHER and G. P. F. SCHMUTH, *Schweiz. Monatsschr. Zahnmed.* **102** (1992) 1195.
8. R. D. BARRET, S. E. BISHARA and J. K. QUINN, *Am. J. Orthod. Dentofac. Orthop* **103** (1993) 8.
9. M. XUE and W. JIA, in Proceedings of the International Symposium on Shape Memory Alloys, Guillin, China 1986, p. 411.
10. X. ZANG, G. LIU, J. YUEN, Q. ZAO, L. YI, Z. HU, S. ZHOU and J. HUO, in Proceedings of the International Symposium on Shape Memory Alloys, Guillin, China 1986, p. 416.

11. J. P. MOFFA, *Calif. Dent. Assoc. J.* **12** (1984) 45.
12. INTERNATIONAL AGENCY FOR RESEARCH ON CANCER, ''Monographs on the evaluation of carcinogenic risk of chemicals to humans'' (IARC, Lyon, France, 1996).
13. L. S. CASTLEMAN and S. M. MOTZKIN, in ''Biocompatibility of clinical implant materials'' edited by D. F. Williams (CRC Press Boca Raton, FL, 1981) p. 129.
14. M. R. GRIMSDOTTIR, A. HENSTEN-PETTERSEN and A. KULLMANN, *Biomaterials* **15** (1994) 1157.
15. J. BACHMANN, *Fortschr. Kieferorthop.* **48** (1987) 492.
16. L. TROMBELLI, A. VIRGILI, M. CORAZZA and R. LUCCI, *Contact Dermatitis* **27** (1992) 259.
17. N. K. VEIEN, E. BORCHHORST, T. HATTEL and G. LAURBERG, *ibid.* **30** (1994) 210.
18. T. FRIES, C. BOURAUEL, D. DRESCHER and R. PLIETSCH, *Fresenius J. Anal. Chem.* **353** (1995) 427.
19. R. P. KUSY, J. Q. WHITLEY, M. J. MAYHEW and J. E. BUCKTHAL, *Angle Orthod.* **58** (1988) 33.
20. J. GEIS-GERSTDORFER and H. WEBER, *Dtsch. Zahnärztl. Z.* **40** (1985) 87.
21. J. M. MEYER and J.-N. NALLY, *J. Dent. Res.* **54** (1975) 678 (Abstract).
22. G. BINNIG, H. ROHRER and C. GERBER, *Appl. Phys. Lett.* **40** (1982) 178.

Received 13 July
and accepted 14 July 1998